J Neurochem. Author manuscript; available in PMC 2016 December 13.

Published in final edited form as:

J Neurochem. 2009 May ; 109(4): 1129–1143. doi:10.1111/j.1471-4159.2009.06045.x.

The atypical protein kinase C in *Aplysia* can form a protein kinase M by cleavage

Joanna K. Bougie[*], **Travis Lim**[†], **Carole Abi Farah**[†], **Varsha Manjunath**[†], **Ikue Nagakura**[*], **Gino B. Ferraro**[†], and **Wayne S. Sossin**[*,†]

[*]Department of Psychology, Montreal Neurological Institute, McGill University, Montreal, Quebec, Canada

[†]Department of Neurology and Neurosurgery, Montreal Neurological Institute, McGill University, Montreal, Quebec, Canada

Abstract

In vertebrates, a brain-specific transcript from the atypical protein kinase C (PKC) ζ gene encodes protein kinase M (PKM) ζ, a constitutively active kinase implicated in the maintenance of synaptic plasticity and memory. We have cloned the atypical PKC from *Aplysia*, PKC *Apl* III. We did not find a transcript in *Aplysia* encoding PKMζ, and evolutionary analysis of atypical PKCs suggests formation of this transcript is restricted to vertebrates. Instead, over-expression of PKC *Apl* III in *Aplysia* sensory neurons leads to production of a PKM fragment of PKC *Apl* III. This cleavage was induced by calcium and blocked by calpain inhibitors. Moreover, nervous system enriched spliced forms of PKC *Apl* III show enhanced cleavage. PKC *Apl* III could also be activated through phosphorylation downstream of phosphoinositide 3-kinase. We suggest that PKM forms of atypical PKCs play a conserved role in memory formation, but the mechanism of formation of these kinases has changed over evolution.

Keywords

Aplysia; atypical PKCs; calpain; learning and memory; protein kinase C; protein kinase M

Experience induced changes in the strength of synapses are thought to be the biochemical mechanism underlying behavioral forms of learning and memory. At the cellular level, multiple memory traces are formed after experiences that last for different amounts of time (Sossin 2008). An attractive model to study these memory traces is the sensory-motor neuron synapse of *Aplysia californica*. Increases in the strength of this synaptic connection occur after learning and contribute to the memory of behavioral sensitization (Kandel 2001). Moreover, these increases can be recapitulated in sensory-motor neuron cultures after addition of serotonin (5HT) (Montarolo *et al.* 1986), the same transmitter used in behavioral sensitization (Glanzman *et al.* 1989).

Address correspondence and reprint requests to Wayne S. Sossin, Department of Neurology and Neurosurgery, Montreal Neurological Institute, McGill University, 3801 University Street, Montreal, QC H3A-2B4, Canada. wayne.sossin@mcgill.ca.

Protein kinase Cs (PKCs) play major roles in both the induction and the maintenance of molecular traces (Sossin 2007). The two phorbol ester-activated PKC isoforms, the classical PKC *Apl*I and the novel PKC *Apl*II play different roles in different memory processes. 5HT translocates PKC *Apl* II at sensory-motor neurons synapses and this activation is important for the ability of 5HT to reverse synaptic depression, a process linked to behavioral dishabituation (Zhao *et al.* 2006; Manseau *et al.* 2001). 5HT alone does not translocate PKC *Apl*I in sensory neurons, however, coupling 5HT and activity results in translocation of PKC *Apl*I in sensory neurons. Also, PKC *Apl*I activity, but not PKC *Apl* II, is important for the induction phase of activity-dependent intermediate facilitation in sensory neurons, which is a process linked to site-specific conditioning in *Aplysia* (Zhao *et al.* 2006; Sutton *et al.* 2001). PKC *Apl*I, but not PKC *Apl* II, has also been implicated in operant conditioning in B51 cells (Lorenzetti *et al.* 2008).

Persistent activation of protein kinases is important for the maintenance of molecular traces that last for longer periods of time, in both *Aplysia* and vertebrates. In *Aplysia*, persistent activation of PKC is implicated in the intermediate-term facilitation that is seen after coupling 5HT and activity (Sutton *et al.* 2001). In vertebrates, a persistently active form of PKCζ [protein kinase M (PKM) ζ] is necessary and sufficient for the maintenance phase of long-term potentiation, and an inhibitor of PKMζ is able to reverses *in-vivo* long-term potentiation and produce persistent loss of behavioral memory at time points where the memories are assumed to be consolidated (Ling *et al.* 2002; Pastalkova *et al.* 2006; Sacktor 2008; Serrano 2005). Furthermore, PKMζ is generated by translation of a unique mRNA whose transcription starts in an intron of PKCζ (Hernandez *et al.* 2003).

In the present paper, we characterize the atypical PKC from *Aplysia*, *Apl* III. We do not find evidence for a PKM form generated by an alternative transcriptional start site, but do provide evidence for cleavage of PKC *Apl* III by calpain, and that alternative splicing in the hinge domain generates a more efficient cleavage site. We also demonstrate that 5HT can regulate PKC *Apl* III though phosphorylation. Together these data suggest that PKC *Apl* III is an attractive candidate for mediating synaptic plasticity in *Aplysia*.

Experimental procedures

Animals

Aplysia californica (75–125 g) were obtained from Marine Specimens Unlimited (Pacific Palisades, CA, USA), and the Mariculture Facility of the University of Miami (Miami, FL, USA). The animals were then maintained in a salt water aquarium until experimentation.

Constructs

Degenerate PCR was used to clone a fragment of PKC *Apl* III using the primers 5′ CCNGARGARCAYGCNMG (256× degeneracy coding for PEEHAR) and the 3′ primer AANAYYGAYTCRTC-NGT (256× degeneracy coding for TEDYLF). A series of 5′ and 3′ rapid amplification of cDNA ends (RACE) reactions were then made using primers from this fragment until the ends of the coding region were reached. One of the 5′RACE reactions was missing the splice inserts, and the presence of splicing was confirmed by additional

PCRs that spanned the spliced region. Additional 5′RACE reactions were also done to test for the presence of alternative start sites in the hinge domain, in the C1 domain and the pseudosubstrate, but no additional sequences were found. To obtain full length sequences for expression constructs, primers were generated with *Bam*HI and *Eco*R1 sites at the end to amplify the full length sequence of PKC *Apl* III using PCR, and the amplified fragment was inserted into the BBACHis2 vector at *Bam*HI and *Eco*R1 sites. Two independent PCRs were sequenced for the reference supplied to GENBANK (Accession number FJ869890). A PKC *Apl* III (No Splice) was generated by amplifying a region surrounding the splice site from gill mRNA and inserting it into the unique sites *Nde*I and *Aat*II in the BBACHis2-PKC *Apl* III construct. In this vector, a kinase dead form was made mutating lysine 297 to arginine using overlap PCR (K297-R). A PKM version of PKC *Apl* III was also constructed using a primer beginning in front of the splice inserts. To generate monomeric red fluorescent protein (mRFP)-tagged PKC *Apl* IIIs in plasmid for neuronal expression 3, all constructs were excised from the BBACHis2 vector with *Bam*HI and *Hind*III; the sites were then filled in with Klenow and inserted into plasmid for neuronal expression 3-mRFP cut with *Sal*I.

Antibodies

The following peptides were synthesized (Invitrogen, Carlsbad, CA, USA) for antibody production and purification: N-terminal VTNTKNDVKYPDGFC-amide; C-terminal, FEYVNPLLMSED-CV-COOH; Splice, CEDHFVDAESFMTAK-amide. For the phospho-specific antibody, the phospo KPGDTTG[pT]FC-amide and corresponding non-phosphorylated peptide were synthesized (Quality controlled biochemicals, Hopkinton MA, USA). Peptides were coupled to bovine serum albumin-Maleimide and Sulfo-link (Pierce, Rockford, IL, USA) according to manufacturer's instruction. For the Splice antibody, cysteines was added to the sequence at the N-terminal, but for the other antibodies cysteines in the coding sequence were used. After conjugation to bovine serum albumin-Maleimide, rabbits were injected with the adjuvant Titer-max and after three boosts the final serum was affinity purified on Sulfo-link columns. For the phospho-specific antibody, the serum was first absorbed on a column containing the non-phosphorylated column and the eluate was affinity purified on the phospho-specific column (Sossin 2003). The antibodies that were used for the subsequent experiments are as follows: a C-terminal antibody (Ab) at a 1 : 1500 concentration, N-terminal Ab at a 1 : 1500 concentration, splice Ab at a 1 : 1500 concentration, and a phospho-specific Ab at a 1 : 400 concentration. In addition, a FITC-goat anti-rabbit green secondary antibody (Zymed Laboratories Inc., South San Francisco, CA, USA), used at a 1 : 40 concentration was used in order to visualize the primary antibodies.

PKC *Apl* III calpain assays

Protein kinase C *Apl* III was purified from baculovirus, according to the protocol outlined in (Lim and Sossin 2006). Purified *Apl* III was then incubated with purified calpain-1 (Calbiochem, San Diego, CA, USA) at varying concentrations for 30 min at 30°C, along with 5×Buffer (2 M $CaCl_2$, 500 mM cystein, 1 M imidazole). Samples were then loaded onto an sodium dodecyl sulfate–polyacrylamide gel electrophoresis (SDS–PAGE) gel and either stained with Coomassie or transferred to a nitrocellulose membrane for western blot analysis with antibodies to *Apl* III.

Aplysia cell cultures and DNA microinjection

Aplysia dissociated sensory neuron cultures were prepared according to the protocol outlined in (Zhao *et al.* 2006), with slight modifications. Individual neurons were pulled from de-sheathed pleural ganglia and isolated in L15 media (Sigma, St Louis, MO, USA) containing 25–50% *Aplysia* hemolymph and plated on coverslips pre-treated with poly-L-lysine (BD Biosciences, San Jose, CA, USA). The cells were then left to attach to the coverslips for a two day period prior to injection.

Solutions of the construct of interest at various concentrations were prepared in filtered double-distilled water and 0.5% fast green dye. The solutions were loaded into glass micropipettes, and the tip of the micropipette was then inserted into the cell nucleus. Short pressure pulses were delivered until the nucleus became uniformly green. Following injection, the cells were kept at 19°C and treatment with various reagents was performed one to three days post-injection. The cells were then fixed and stained for immunocytochemistry.

Immunocytochemistry

Following treatment with the reagents, the cells were fixed for 30 min in 4% paraformaldehyde in 30% sucrose, 1×phosphate-buffered saline (PBS). In order to permeabilize the cells, they were washed in 0.1% Triton X-100 in 30% sucrose, 1×PBS for 10–15 min. The cells were then washed three times in 1×PBS, and washed again in NH_4Cl for 15 min to quench free aldehydes. Prior to addition of the antibodies, the cells were blocked for 30 min in 10% normal goat serum in 0.5% Triton X-100, 1×PBS. Samples were then incubated with various primary antibodies diluted in the blocking solution for 1 h, washed four times with 1×PBS, and then treated in the dark with a secondary green fluorescent antibody; FITC-Goat Anti-Rabbit IgG (Zymed Laboratories) at a concentration of 1 : 40 diluted in the blocking solution. Cells were washed again in 1×PBS, and finally mounted on slides using Dako fluorescent mounting media (DakoCytomation, Glostrup, Denmark).

Confocal microscopy and image quantification

Neurons expressing the mRFP constructs were imaged using a laser scanning confocal microscope (Zeiss Canada, Toronto, ON, Canada), and pictures were captured using the 40× objective at the middle of the cell where the nucleus was as well defined as possible. Within each experiment the same laser power was used for all groups. Pictures were then opened in the IP Lab (BD Biosciences) analysis program, and the perimeter of the cell was either identified automatically (high expressing cells) or manually outlined (lower expressing cells). The density of concentric rings one pixel in width from the perimeter to the center of the cell body was measured as described (Zhao *et al.* 2006; Nagakura *et al.* 2008). The cytoplasm was defined as between 10 and 20 pixels inward from the perimeter while the last five inward pixels were defined as the nucleus. While the procedure was automated, visual inspection of all cells confirmed that these regions corresponded to the cytoplasm and nucleus of each cells. Fluorescence ratios were then calculated. For normalized ratios, the nuclear/cytoplasmic ratio was divided by the average nuclear/cytoplasmic ratio of control cells. Normalization was important for including multiple independent experiments from

independent batches of sensory cells as there was some variability in the control nuclear/cytoplasmic ratio between different batches of sensory cells.

To quantify phosphorylation, the ratio of phospho-specific antibody staining to mRFP expression in the cytoplasm was measured for each cell. The data were normalized by dividing both control and experimental ratios by the average ratio of control cells in each experiment.

Results

Cloning of PKC *Apl* III

We cloned the full-length sequence of the atypical PKC from *Aplysia*, using degenerate PCR and RACE (see Methods), which will now be referred to as PKC *Apl* III. Examination of the trace archives of the *Aplysia* genome and available cDNA repositories did not indicate the presence of additional atypical PKCs. Like all atypical PKCs, PKC *Apl* III has a Phox and Bem 1 (PB1) domain followed by the pseudosubstrate, an atypical C1 domain, a hinge domain and the kinase domain, and all of these domains are highly conserved (Fig. 1a). Using the genome trace archive we have defined the exons of PKC *Apl* III, and the exon-intron usage is also highly conserved with vertebrate PKCs with a few exceptions (Fig. 1b). Interestingly, one unique feature of PKC *Apl* III is the presence of two alternatively used exons in the hinge domain (Fig. 1b).

Is there an alternative mRNA encoding PKMζ in *Aplysia*?

In vertebrates, there is an alternative transcriptional start site between exons 4 and 5 that generates an mRNA that encodes PKMζ. Using 5′ RACE, we were unable to detect any mRNAs containing an alternative start site. In vertebrates, there are two forms of atypical PKC, PKCζ and PKCι, but only PKCζ has a transcriptional start site between exons 4 and 5. A strong evolutionary constraint for the alternative transcript is the initiating methionine for PKMζ. Indeed, the initiating methionine, present at the end of exon 5, is present in all vertebrate orthologues of PKCζ, even in primitive fishes such as Tetraodon, but is not present in any PKCι (Fig. 1c). Moreover, examining the atypical PKCs in the deuterostome lineages that diverged before vertebrates, where only one atypical PKC is present, the methionine is also absent, suggesting this methionine originated after the duplication into distinct PKCζ and PKCι isoforms. The methionine is also absent in invertebrate atypical PKCs, including PKC *Apl* III (Fig. 1c).

Another feature of the presence of the alternative start site is homology in the intron, both because of the transcriptional promoter and the sequence of the 5′UTR. Unlike the long intron present in vertebrate PKCs, the intron in *Aplysia* between exons 4 and 5 is only 440 bp long. We looked for homology in this intron from PKC *Apl* III to vertebrate PKCs and no significant homology was detected. We also examined the intron between exon 4 and exon 5 in the genomic region of the more-closely related mollusk *Lottia.* Again, no homologous region was found in the intron. In contrast, homology was seen between primitive fishes, mice and human in this region (Hernandez *et al.* 2003; data not shown).

There has been some discussion of an atypical PKM in *Drosophila* (Drier *et al.* 2002). The intron/exon boundaries of the critical exons around the transcriptional start site are conserved in *Drosophila*. Examination of the *Drosophila* database does show evidence for alternative transcriptional start sites in an intron of the *Drosophila* atypical PKC, but these are all in the intron preceding the equivalent of exon 4, not between the equivalent of exons 4 and 5. These transcripts encode proteins with an initiating methionine before the pseudosubstrate sequence, indicating that they may not encode PKMs. It is conceivable that these methionines are skipped and that these transcripts do encode an atypical PKM, but this would be an example of convergent evolution because of a new transcriptional start site and a new initiating methionine, not conservation of an ancient transcript.

While it is difficult to prove the absence of a molecule, based on bioinformatics analysis of a number of genomes, it is unlikely that the formation of a PKM form of the atypical PKC by an alternative start site is conserved in invertebrates. Instead, it appears likely that it arose during the duplication of atypical PKCs in the early vertebrate lineage.

PKC *Apl* III contains two alternatively spliced inserts in the hinge domain that are enriched in the nervous system

While cloning PKC *Apl* III we noted that there were two alternative exons not present in all transcripts (Fig. 2a). To determine the abundance of messages that contained inserts we took advantage of restriction sites present in each exon (Fig. 2). We amplified a fragment of PKC *Apl* III using PCR from either nervous system, gill, or ovotestis. We then cut these fragments with *Taq*I to identify fragments containing exon 8a, *Fok*I to identify fragments containing 8b and *Bgl*II to confirm the identity of the amplified fragment. All fragments cut completely with *Bgl*II to confirm amplification of PKC *Apl* III in all tissues. In the gill, there was no detectable cleavage with *Fok*, and *Taq*I cut only in the non-spliced region suggesting minimal inclusion of these exons in the gill. In ovotestis, there was no detectable cleavage with *Fok*I, but about 50% of the amplified fragments cut with *Taq*I, suggesting partial inclusion of exon 8a. In the nervous system, a high percentage of the fragments cut with both *Fok*I and *Taq*I signifying that most fragments contain both exons. This was confirmed by sequencing multiple amplifications demonstrating clones contain 8a alone, 8b alone or both 8a and 8b. The inclusion of exons specifically in the nervous system fragment can also be seen by the larger size of the lower *Bgl* II fragment in the nervous system digest (Fig. 2b).

To confirm that the protein encoded by these exons was produced, we raised three antibodies to PKC *Apl* III: one to the carboxy-terminal (C-terminal), one to the PB1 domain (N-terminal) and one specific to exon 8b (Splice), and compared immunoreactivity between the nervous system and the gill. The antibody to the C-terminal recognized a major band of approximately 70 kDa in the nervous system, while the major immunoreactive band in the gill migrated faster at approximately 67 kDa. Similar bands were seen with the N-terminal antibody. The Splice antibody recognized only the higher molecular weight species and moreover, its relative intensity was much higher in the nervous system than the gill. This confirms the enrichment of the isoform with the splice sites in the nervous system. While the PCR results did not detect PKC *Apl* III with inserts in the gill, the antibody to the splice site did recognize a protein with the splice site. This may be because of better sensitivity of the

immuoblots. Alternatively, if nervous system processes innervate the gill, they may contain PKC *Apl* III protein detectable by immunoblotting in the absence of any mRNA encoding PKC *Apl* III which could be restricted to the cell bodies of the innervating neurons.

Over-expression of PKC *Apl* III in *Aplysia* sensory neurons induces cleavage of PKC *Apl* III

We generated a tagged form of PKC *Apl* III by creating a plasmid encoding mRFP fused to the N-terminal of PKC *Apl* III, mRFP-PKC *Apl* III. We have previously generated similar fusions for PKC *Apl*I and PKC *Apl* II that retain biological activity (Manseau *et al.* 2001). We initially expressed this construct in SF9 cells, and this construct was shown to be expressed in the cytoplasm, but was not translocated to membranes by dioctanoylglycerol or phorbol esters (Fig. 3a; data not shown). In similar experiments both PKC *Apl*I and PKC *Apl* II were translocated (Zhao *et al.* 2006; Farah *et al.* 2008). The lack of PKC *Apl* III translocation was expected as the atypical C1 domain of these PKCs does not bind diacylglycerol or phorbol esters (Chen 1993). mRFP-PKC *Apl* III was next over-expressed in cultured *Aplysia* sensory neurons. Unlike SF9 cells, confocal images revealed that mRFP is strongly expressed in the nucleus as well as the cytoplasm in sensory neurons (Fig. 3b) This is a surprising result, as mRFP is not seen in the nucleus when similarly tagged versions of PKC *Apl*I or PKC *Apl* II are over-expressed (Zhao *et al.* 2006 and Fig. 3b). Additionally, under live imaging conditions, mRFP-PKC *Apl* III still expresses in the nucleus of sensory neurons, signifying that the nuclear expression is not simply because of an effect of cell fixation (data not shown).

We then immunostained cells expressing mRFP-PKC *Apl* III using the antibody to the C-terminal. Surprisingly, staining with the antibody was not enriched in the nucleus similar to the mRFP, suggesting separation of the N-terminal containing mRFP and the C-terminal recognized by the antibody, presumably by endoproteolytic cleavage (Fig. 3c and d). The difference between mRFP staining and antibody staining was not because of recognition of the endogenous protein by the antibody, since at the laser power used for these images, no staining was observed in un-injected cells (Fig. 3d). We were concerned that during cloning, we may had introduced a cleavage site between mRFP and PKC *Apl* III, and to rule this out, immuno-stained with the N-terminal antibody. This antibody showed significantly more staining in the nucleus, inconsistent with cleavage in the linker between mRFP and PKC *Apl* III, but consistent with cleavage somewhere after the PB1 domain (Fig. 3e and f). We next examined endogenous staining of PKC *Apl* III using higher laser power. The staining resembled mRFP staining being distributed equally between the cytoplasm and the nucleus (Fig. 3d). Thus, it appears that in *Aplysia* sensory neurons but not SF9 cells, PKC *Apl* III can localize to the nucleus. Moreover, when expressed at high levels, PKC *Apl* III is cleaved with the N-terminal continuing to localize to both the nucleus and the cytoplasm, but with the C-terminal restricted to the cytoplasm. This is consistent with the signals for nuclear shuttling being present in the N-terminal region. Thus, after cleavage the C-terminal fragment redistributes into the cytoplasm while the N-terminal fragment continues to shuttle between the cytoplasm and the nucleus (Fig. 4).

Cleavage is more efficient with the splice inserts

Upon further examination, we found that the putative cleavage is sensitive to levels of *Apl* III: diluting the concentration of injected mRFP-PKC *Apl* III DNA revealed that the lower expressing cells show no differences between mRFP staining and staining with an antibody to the C-terminus (Fig. 4). Indeed, both are now equally distributed between the cytoplasm and the nucleus. To quantify cleavage, we used the nuclear/cytoplasmic ratio of immunofluorescence with the C-terminal antibody, reasoning that after cleavage the C-terminal catalytic domain no longer localizes to the nucleus (Fig. 4). At low levels of expression the staining with the antibody and mRFP were similar leading to a ratio near to 1. At high levels of expression, immunostaining in the nucleus greatly decreased leading to a ratio close to 0.3 (Fig. 4). There is a fairly steep relationship between the level of over-expression and cleavage: no cleavage is observed at low levels of expression, and almost complete cleavage is seen as mRFP levels increase over a 2–4 fold level of expression (Fig. 4).

The splice inserts are in the hinge domain and may affect cleavage. Thus, we generated an mRFP-PKC *Apl* III lacking the splice inserts (No-Splice) and compared the amount of cleavage by comparing the nuclear/cytoplasmic ratio of the two constructs (Fig. 5a and b). Splicing does not affect expression of mRFP in the nucleus and is not required for cleavage, as at high levels of mRFP-PKC *Apl* III expression there is no difference in the nuclear/cytoplasmic ratio in cells with high levels of mRFP (Fig. 5c). Similarly, at low levels of expression neither mRFP-PKC *Apl* III is cleaved. However, at intermediate levels of expression there is a significant difference in the nuclear/cytoplasmic ratio of mRFP-PKC *Apl* III and mRFP-PKC *Apl* III (No-Splice), suggesting that the splice sites increase the rate or efficiency of cleavage (Fig. 5b; values of individual cells in 5a; overall data in 5c). Importantly, in this intermediate stage, the levels of expression of the two constructs were not different (Fig. 5d).

Cleavage is sensitive to inhibitors of Calpain

Cleavage of PKC to a PKM is often mediated by calpain (Pontremoli *et al.* 1990; Sessoms *et al.* 1992). To determine if the cleavage induced by over-expression was also mediated by calpain, sensory neurons were injected with a high concentration (0.3 μg/μL) of the mRFP-PKC *Apl* III. One hour post-injection, cells were treated with either Calpain Inhibitor V (100 μM), a cell-permeable, irreversible, non-specific inhibitor of calpains, or a vehicle solution. The cells were left to express over-night in their respective solutions, and were then fixed the next day for immunocytochemistry. As indicated in Fig. 6, the calpain inhibitor was able to significantly block the over-expression induced cleavage of mRFP-PKC *Apl* III. This can be seen in the significantly higher green nuclear/cytoplasmic ratio when compared to the vehicle condition. Similar results were also seen using calpeptin, where the inhibitor was replenished in applications every hour since this inhibitor is reversible (data not shown). In contrast, no inhibition of cleavage was seen with caspase inhibitors (data not shown). While levels of calcium are relatively low in resting sensory neurons, calpain activity has been detected in *Aplysia* neurons without stimulation in previous studies (Gitler and Spira 1998; Khoutorsky and Spira 2008).

PKC *Apl* III splice inserts provide a site for cleavage by calpain *in vitro*

To determine directly if PKC *Apl* III cleavage by calpain was regulated by the splice inserts, we purified PKC *Apl* III with the splice inserts (Wild-Type) and PKC *Apl* III without the splice inserts (No-Splice) from SF9 cells infected with baculovirus encoding these isoforms, and subsequently performed *in-vitro* cleavage reactions with purified calpain. While the PKC *Apl* III No-Splice is still cleaved by calpain, the splice inserts provide for more efficient cleavage (Fig. 7). This is consistent with the results in intact cells where the isoform without the spliced site is cleaved, but less efficiently. Notably, the pattern of cleavage seen by Coomassie staining indicated that the major cleavage site was different in the kinase with the splice inserts: the major band seen after cleaving PKC *Apl* III Wild-Type (arrow) migrated slightly below the 50 kDa marker, at a lower molecular weight than the major band seen after cleavage of PKC *Apl* III No-Splice (squiggly arrow). There is also a minor band seen after cleaving PKC *Apl* III Wild-Type that migrated above the band seen after cleavage of PKC *Apl* III No-Splice, consistent with a fragment cut at the same site as PKC *Apl* III No-Splice but containing the splice inserts (arrowhead). All these fragments are immunoreactive with the C-terminal antibody and phospho-specific antibody (Fig. 7). Additionally, N-terminal fragments were not observed (N-terminal antibody; data not shown), presumably they were unstable under these conditions. The size of the major C-terminal fragment seen after cleavage of PKC *Apl* III Wild-Type is consistent with cleavage at or near the splice inserts (see schematic in Fig. 7). Supporting this idea, these fragments were not observed using the splice-specific PKC *Apl* III antibody; instead only the minor fragment, probably cleaved at the same site as observed in the PKC *Apl* III No-Splice case was immunoreactive (arrowhead). The purified PKC *Apl* III No-Splice also does not react with the splice-specific PKC *Apl* III antibody, further confirming the specificity of the antibody itself.

Activity dependent cleavage of PKC *Apl* III can be induced by increasing intracellular levels of Ca^{2+}

As cleavage by calpain is usually calcium-dependent, we examined whether cleavage could be induced in cells having a low amount of mRFP-PKC *Apl* III expression using the calcium ionophore, ionomycin. Initial experiments examining the nuclear/cytoplasmic ratio immediately after ionomycin revealed no effect (data not shown). However, if cleavage occurred in the cytoplasm, a change in the redistribution of mRFP-PKC *Apl* III would not be observed immediately; there would be a lag time until the remaining uncleaved mRFP-PKC *Apl* III redistributed into the cytoplasm, while the now cleaved cytoplasmic form of mRFP-PKC *Apl* III would not redistribute. Indeed, 2 h after ionomycin treatment a small but highly significant decrease in the nuclear/cytoplasmic ratio was observed (Fig. 8). Interestingly, the ratio was not changed in the lowest expressing cells, suggesting that cleavage required both calcium influx and a moderate level of mRFP-PKC *Apl* III expression (Fig. 8).

PKC *Apl* III is phosphorylated downstream of 5HT

Atypical PKCs are regulated by phosphorylation in the catalytic domain. In particular, phosphorylation of a site in the activation loop of atypical PKCs by a phosphoinositide-3 kinase (PI3K)-dependent phosphoinositide-dependent kinase (PDK) 1 mechanism is known

to control their activation (Chou *et al.* 1998). In *Aplysia*, there is indirect evidence that 5HT activates PI3K, as a number of 5HT-mediated processes including activation of target of rapamycin, synthesis of sensorin, and induction of morphological changes are blocked by inhibitors of PI3K (Khan *et al.* 2001; Udo *et al.* 2005; Hu *et al.* 2006).

To investigate regulation of PKC *Apl* III by PI3K and PDK, we raised a phospho-specific antibody to PKC *Apl* III at the PDK site. This antibody recognized expressed PKC *Apl* III, but not a glutathione-S-transferase (GST)-PKM *Apl* III fragment that should not be phosphorylated as it was isolated from bacteria (Fig. 9a). While this antibody recognized multiple bands on immunoblots, it could be used to recognize the expressed PKC *Apl* III since, similar to the other antibodies, a laser power was used to detect the over-expressed protein where no immunoractivity was detected in non-expressing cells. To examine phosphorylation, we used a 10 min application of 5HT, as unlike a 5 min application of 5HT, 10 min applications of 5HT leads to facilitation that is more dependent on PKC (Hawkins *et al.* 2006). When mRFP-PKC *Apl* III was expressed at low levels in *Aplysia* sensory neurons, 5HT increased phosphorylation at the PDK site (Fig. 9b and c). However, at higher levels of expression when mRFP-PKC *Apl* III was cleaved, there was no effect of 5HT on the phosphorylation at the PDK site (Fig. 9c). This result is in agreement with a study on mammalian PKMζ, where PDK phosphorylation of PKMζ was constitutive because of the increased access of PDK to the phosphorylation site in the absence of the regulatory domain (Kelly *et al.* 2007). 5HT phosphorylation of mRFP-PKC *Apl* III was also shown to be downstream of the PI3K-PDK pathway, as it was blocked by LY 294002, an inhibitor of PI3K (Fig. 9d).

Discussion

There has been rising interest in the PKM form of atypical PKCs because of their potential role as a memory trace in vertebrate learning (Ling *et al.* 2002; Serrano *et al.* 2005; Pastalkova *et al.* 2006; Kelly *et al.* 2007; Shema *et al.* 2007; Sacktor 2008; Sossin 2008). Here, we show that while the mechanism of formation of the atypical PKM may have changed over evolution, the presence of an atypical PKM may be conserved.

Activation of cleavage by over-expression

Why does over-expression lead to cleavage? The simplest explanation is that normally PKC *Apl* III is protected from cleavage by an endogenous protein. When expression of PKC *Apl* III reaches a high enough level that it titrates out this protein, it is then available for cleavage by calpain. This does not appear to be because of increased phosphorylation by PKC *Apl* III, as a kinase dead PKC *Apl* III with the catalytic lysine converted to arginine is still cleaved (data not shown). One candidate for this protective protein are heat shock proteins, HSP70 for example is known to protect non-phosphorylated PKCs from degradation (Gao and Newton 2006). It is possible that regulation of this protein at specific sites to remove its protection could be a mechanism for regulation of PKC *Apl* III cleavage.

Is there a physiological role for PKM *Apl* III in *Aplysia*?

Using an over-expression paradigm, we have been able to detect cleavage of the atypical PKC *Apl* III; however to be physiologically important, cleavage of the endogenous PKC *Apl* III is required. Cleavage is highly dependent on the level of expression, and this may explain the inability to detect the endogenous PKM form of PKC *Apl* III using immunoblots (data not shown). Thus, if endogenous PKC *Apl* III is to be cleaved, it would have to be a local event either because of high local levels of PKC *Apl* III, or a regulated removal of the chaperone that prevents cleavage at normal expression levels. While this could conceivably be detected by immunohistochemistry, we do not have an antibody that detects only PKM *Apl* III and not PKC *Apl* III and thus cannot detect PKM formation locally at synapses. Moreover, our present ability to detect cleavage is slow and insensitive because of the requirement for nuclear shuttling to detect cleavage. A more sensitive method of detection will be required to detect the local cleavage that is likely to by physiologically important.

There are two paradigms where persistent activation of PKC downstream of calpain is important for memory in *Aplysia*. The first is after site-specific sensitization or after pairing 5HT and activity (Sutton *et al.* 2001, 2004). While in this case, PKC *Apl*I is required for the induction of facilitation in this paradigm (Zhao *et al.* 2006), it is not clear what isoform of PKC is required for the maintenance of facilitation, and it may be PKM *Apl* III. The second paradigm is in the motor neuron, where an increase in enhancement of the glutamate-evoked potential (Glu-EP) by 5HT depends on both rapid protein synthesis and calcium (Li *et al.* 2005; Villareal *et al.* 2007). Importantly, PKC inhibitors block both the induction and the maintenance of the increased Glu-EP (Villareal *et al.* 2009). In particular, the maintenance of this sensitivity to glutamate is blocked by small concentrations of chelerythrine, but not small concentrations of Bis, and this matches the pharmacological profile of purified PKM *Apl* III (Villareal *et al.* 2009). Finally, the 5HT mediated increase in the Glu-EP is blocked by calpain, consistent with cleavage of PKM *Apl* III being required for this effect (Villareal *et al.* 2009). Indeed, PKC *Apl* III is also cleaved by over-expression in *Aplysia* motor neurons (data not shown). Thus, it is likely that physiological cleavage of PKC *Apl* III by calpain underlies the increase in the Glu-EP seen after 5HT treatment, and this increase is important for behavioral sensitization (Li *et al.* 2005; Glanzman 2008).

Is PKM formation specific for PKC *Apl* III?

Both PKC *Apl*I and *Apl* II can be cleaved *in-vitro* by calpain to form a PKM (Sutton *et al.* 2004), as is PKC *Apl* III (Fig. 7). Since PKC *Apl*I and PKC *Apl* II do not shuttle through the nucleus, the assay we are using to detect cleavage for PKC *Apl* III is not valid for PKC *Apl*I and PKC *Apl* II. However, the normal translocation of enhanced green fluorescent protein-PKC *Apl*I and enhanced green fluorescent protein-PKC *Apl* II are not consistent with a large amount of cleavage occurring. However, we cannot rule out that PKC *Apl*I and PKC *Apl* II are also cleaved by calpain and that PKMs may be formed from distinct isoforms of PKC depending on the type of stimulation.

Nuclear shuttling of PKC *Apl* III

Unlike PKC *Apl*I or PKC *Apl* II, both endogenous and tagged forms of PKC *Apl* III are found in the nucleus. There have been previous reports of nuclear PKCs including atypical

forms (Zhou *et al.* 1997), but the role of nuclear PKCs are not clear. The sequences found to be important for nuclear import in the C1 domain of atypical PKCs (Perander *et al.* 2001) and the leucine rich sequence preceding the catalytic domain encoding nuclear export of atypical PKCs (Perander *et al.* 2001) are completely conserved in PKC *Apl* III. Thus, nuclear shuttling is a highly conserved feature of atypical PKCs. PKC *Apl* III expressed in heterologous SF9 cells is not found in the nucleus, suggesting that some protein expressed in *Aplysia* neurons but not SF9 cells is required for the nuclear localization of PKC *Apl* III. Indeed, the nuclear import sequence in atypical PKCs does not match the classical nuclear import signals and may require additional proteins for function (Perander *et al.* 2001).

Activation of PKC *Apl* III phosphorylation by 5HT

Protein kinase C ζ has been shown to be downstream of PI3K through the phosphorylation of the active loop of the kinase in many different systems (Hirai and Chida 2003). Here, we also show that 5HT, through PI3K activation, increases PKC *Apl* III phosphorylation in sensory cells. 5HT activation of PI3K is thought to be important for activation of the target of rapamycin pathway and through it sensorin translation (Khan *et al.* 2001; Carroll *et al.* 2004, 2006; Hu *et al.* 2006). PI3K is also important for induction of cytoskeletal change (Udo *et al.* 2005). PKCζ thus may play a role in these pathways. The PI3K induction is limited to the intact kinase, as the PKM version, similar to vertebrate PKMζ, appears to be constitutively phosphorylated at that site. If PKM *Apl* III is persistently phosphorylated, it is conceivable that the increase in phosphorylation is downstream of cleavage. However, the phosphorylation is blocked by PI3K inhibitors, and these inhibitors are not known to inhibit calpain.

A conserved physiological role for PKMζ?

It will be interesting to determine if the evolutionary role of the PKMζ in regulating α-amino-3-hydroxy-5-methylisoxazole-4-propionate (AMPA) receptor trafficking is conserved (Yao *et al.* 2008). The ability to generate a separate transcriptional form may have required gene duplication, since the full length atypical PKC has major conserved roles in polarity, including axon determination in the nervous system (Banker 2003). Once the gene had been duplicated, one isoform could be devoted to cell polarity, and the other optimized for PKM formation.

Indeed, as discussed above recent work suggests that in *Aplysia*, increased sensitivity to glutamate after 5HT treatment is because of insertion of AMPA receptors this is likely dependent on the PKM form of PKC *Apl* III (Chitwood *et al.* 2001; Li *et al.* 2005; Villareal *et al.* 2009). Thus, PKM forms of atypical PKCs may have a conserved role in regulating AMPA receptor trafficking; however the mechanism for the production of PKM may have changed over evolution.

Acknowledgments

This work was supported by Canadian Institutes of Health Research (CIHR) Grant MOP 12046 (W.S.S.). C.A.F. is the recipient of a postdoctoral fellowship from the Fonds de la Recherche en Santé du Québec (FRSQ) and W.S.S. is a William Dawson Scholar and an FRSQ Chercheur National.

Abbreviations used

5HT	serotonin
AMPA	α-amino-3-hydroxy-5-methylisoxazole-4-propionate
Glu-EP	glutamate-evoked potential
mRFP	monomeric red fluorescent protein
PB1	Phox and Bem 1
PBS	phosphate-buffered saline
PDK	phosphoinositide-dependent kinase
PI3K	phosphoinositide-3 kinase
PKC	protein kinase C
PKM	protein kinase M

References

Banker G. Pars, PI 3-kinase, and the establishment of neuronal polarity. Cell. 2003; 112:4–5. [PubMed: 12526787]

Carroll M, Warren O, Fan X, Sossin WS. 5-HT stimulates eEF2 dephosphorylation in a rapamycin-sensitive manner in Aplysia neurites. J Neurochem. 2004; 90:1464–1476. [PubMed: 15341530]

Carroll M, Dyer J, Sossin WS. Serotonin increases phosphorylation of synaptic 4EBP through TOR, but eukaryotic initiation factor 4E levels do not limit somatic cap-dependent translation in Aplysia neurons. Mol Cell Biol. 2006; 26:8586–8598. [PubMed: 16982686]

Chen CC. Protein kinase C alpha, delta, epsilon and zeta in C6 glioma cells. TPA induces translocation and down-regulation of conventional and new PKC isoforms but not atypical PKC zeta. FEBS Lett. 1993; 332:169–173. [PubMed: 8405436]

Chitwood RA, Li Q, Glanzman DL. Serotonin facilitates AMPA-type responses in isolated siphon motor neurons of Aplysia in culture. J Physiol. 2001; 534:501–510. [PubMed: 11454967]

Chou MM, Hou W, Johnson J, Graham LK, Lee MH, Chen C-S, Newton AC, Schaffhausen BS, Toker A. Regulation of protein kinase C [zeta] by PI 3-kinase and PDK-1. Curr Biol. 1998; 8:1069–1078. [PubMed: 9768361]

Drier EA, Tello MK, Cowan M, Wu P, Blace N, Sacktor TC, Yin JCP. Memory enhancement and formation by atypical PKM activity in *Drosophila melanogaster*. Nat Neurosci. 2002; 5:316–324. [PubMed: 11914720]

Farah CA, Nagakura I, Weatherill D, Fan X, Sossin WS. Physiological role for phosphatidic acid in the translocation of the novel protein kinase C Apl II in Aplysia neurons. Mol Cell Biol. 2008; 28:4719–4733. [PubMed: 18505819]

Gao T, Newton AC. Invariant Leu preceding turn motif phosphorylation site controls the interaction of protein kinase C with Hsp70. J Biol Chem. 2006; 281:32461–32468. [PubMed: 16954220]

Gitler D, Spira ME. Real time imaging of calcium-induced localized proteolytic activity after axotomy and its relation to growth cone formation. Neuron. 1998; 20:1123–1135. [PubMed: 9655501]

Glanzman DL. New tricks for an old slug: the critical role of postsynaptic mechanisms in learning and memory in Aplysia. Prog Brain Res. 2008; 169:277–292. [PubMed: 18394481]

Glanzman DL, Mackey SL, Hawkins RD, Dyke AM, Lloyd PE, Kandel ER. Depletion of serotonin in the nervous system of Aplysia reduces the behavioral enhancement of gill withdrawal as well as the heterosynaptic facilitation produced by tail shock. J Neurosci. 1989; 9:4200–4213. [PubMed: 2592997]

Hawkins RD, Kandel ER, Bailey CH. Molecular mechanisms of memory storage in Aplysia. Biol Bull. 2006; 210:174–191. [PubMed: 16801493]

Hernandez AI, Blace N, Crary JF, Serrano PA, Leitges M, Libien JM, Weinstein G, Tcherapanov A, Sacktor TC. Protein kinase M{zeta} synthesis from a brain mRNA encoding an independent protein kinase C{zeta} catalytic domain: implications for the molecular mechanism of memory. J Biol Chem. 2003; 278:40305–40316. [PubMed: 12857744]

Hirai T, Chida K. Protein kinase C{zeta} (PKC{zeta}): activation mechanisms and cellular functions. J Biochem. 2003; 133:1–7. [PubMed: 12761192]

Hu J-Y, Wu F, Schacher S. Two signaling pathways regulate the expression and secretion of a neuropeptide required for long-term facilitation in Aplysia. J Neurosci. 2006; 26:1026–1035. [PubMed: 16421322]

Kandel E. Nobel Lecture: the molecular biology of memory storage: a dialog between genes and synapses. Biosci Rep. 2001; 21:565–611. [PubMed: 12168768]

Kelly MT, Crary JF, Sacktor TC. Regulation of protein kinase Mzeta synthesis by multiple kinases in long-term potentiation. J Neurosci. 2007; 27:3439–3444. [PubMed: 17392460]

Khan A, Pepio AM, Sossin WS. Serotonin activates S6 kinase in a rapamycin-sensitive manner in Aplysia synaptosomes. J Neurosci. 2001; 21:382–391. [PubMed: 11160419]

Khoutorsky A, Spira ME. Calpain inhibitors alter the excitable membrane properties of cultured Aplysia neurons. J Neurophysiol. 2008; 100:2784–2793. [PubMed: 18684908]

Li Q, Roberts AC, Glanzman DL. Synaptic facilitation and behavioral dishabituation in Aplysia: dependence on release of Ca2+ from postsynaptic intracellular stores, postsynaptic exocytosis, and modulation of postsynaptic AMPA receptor efficacy. J Neurosci. 2005; 25:5623–5637. [PubMed: 15944390]

Lim T, Sossin WS. Phosphorylation at the hydrophobic site of protein kinase C Apl II is increased during intermediate term facilitation. Neuroscience. 2006; 141:277–285. [PubMed: 16677767]

Ling DSF, Benardo LS, Serrano PA, Blace N, Kelly MT, Crary JF, Sacktor TC. Protein kinase M[zeta] is necessary and sufficient for LTP maintenance. Nat Neurosci. 2002; 5:295–296. [PubMed: 11914719]

Lorenzetti FD, Baxter DA, Byrne JH. Molecular mechanisms underlying a cellular analog of operant reward learning. Neuron. 2008; 59:815–828. [PubMed: 18786364]

Manseau F, Fan X, Hueftlein T, Sossin WS, Castellucci VF. Ca2+-independent protein kinase C Apl II mediates the serotonin-induced facilitation at depressed Aplysia sensorimotor synapses. J Neurosci. 2001; 21:1247–1256. [PubMed: 11160395]

Montarolo PG, Goelet P, Castellucci VF, Morgan J, Kandel ER, Schacher S. A critical period for macromolecular synthesis in long-term heterosynaptic facilitation in Aplysia. Science. 1986; 234:1249–1254. [PubMed: 3775383]

Nagakura I, Ormond J, Sossin WS. Mechanisms regulating ApTrkl, a Trk-like receptor in Aplysia sensory neurons. J Neurosci Res. 2008; 86:2876–2883. [PubMed: 18521934]

Pastalkova E, Serrano P, Pinkhasova D, Wallace E, Fenton AA, Sacktor TC. Storage of spatial information by the maintenance mechanism of LTP. Science. 2006; 313:1141–1144. [PubMed: 16931766]

Perander M, Bjorkoy G, Johansen T. Nuclear import and export signals enable rapid nucleocytoplasmic shuttling of the atypical protein kinase C lambda. J Biol Chem. 2001; 276:13015–13024. [PubMed: 11115515]

Pontremoli S, Melloni E, Sparatore B, Michetti M, Salamino F, Horecker BL. Isozymes of protein kinase C in human neutrophils and their modification by two endogenous proteinases. J Biol Chem. 1990; 265:706–712. [PubMed: 2295614]

Sacktor TC. PKMζ, LTP maintenance, and the dynamic molecular biology of memory storage. Prog Brain Res. 2008; 169:27–40. [PubMed: 18394466]

Serrano P, Yao Y, Sacktor TC. Persistent phosphorylation by protein kinase M{zeta} maintains late-phase long-term potentiation. J Neurosci. 2005; 25:1979–1984. [PubMed: 15728837]

Sessoms JS, Chen SJ, Chetkovich DM, Powell CM, Roberson ED, Sweatt JD, Klann E. Ca(2+)-induced persistent protein kinase C activation in rat hippocampal homogenates. Second Messengers Phosphoproteins. 1992; 14:109–126. [PubMed: 1345337]

Shema R, Sacktor TC, Dudai Y. Rapid erasure of long-term memory associations in the cortex by an inhibitor of PKM{zeta}. Science. 2007; 317:951–953. [PubMed: 17702943]

Sossin WS. Phosphopeptide antibodies to PKC. Methods Mol Biol. 2003; 233:233–244. [PubMed: 12840511]

Sossin WS. Isoform specificity of protein kinase Cs in synaptic plasticity. Learn Mem. 2007; 14:236–246. [PubMed: 17404386]

Sossin WS. Defining memories by their distinct molecular traces. Trends Neurosci. 2008; 31:170–175. [PubMed: 18329733]

Sutton MA, Masters SE, Bagnall MW, Carew TJ. Molecular mechanisms underlying a unique intermediate phase of memory in Aplysia. Neuron. 2001; 31:143–154. [PubMed: 11498057]

Sutton MA, Bagnall MW, Sharma SK, Shobe J, Carew TJ. Intermediate-term memory for site-specific sensitization in Aplysia is maintained by persistent activation of protein kinase C. J Neurosci. 2004; 24:3600–3609. [PubMed: 15071108]

Udo H, Jin I, Kim J-H, Li H-L, Youn T, Hawkins RD, Kandel ER, Bailey CH. Serotonin-induced regulation of the actin network for learning-related synaptic growth requires Cdc42, N-WASP, and PAK in Aplysia sensory neurons. Neuron. 2005; 45:887–901. [PubMed: 15797550]

Villareal G, Li Q, Cai D, Glanzman DL. The role of rapid, local, postsynaptic protein synthesis in learning-related synaptic facilitation in aplysia. Curr Biol. 2007; 17:2073–2080. [PubMed: 18006316]

Villareal G, Li Q, Cai D, Fink A, Lim T, Bougie J, Sossin WS, Glanzman DL. Role of protein kinase C in the induction and maintenance of serotonin-dependent enhancement of the glutamate response in isolated siphon motor neurons of Aplysia. J Neurosci. 2009 In Press.

Yao Y, Kelly MT, Sajikumar S, Serrano P, Tian D, Bergold PJ, Frey JU, Sacktor TC. PKM zeta maintains late long-term potentiation by N-ethylmaleimide-sensitive factor/GluR2-dependent trafficking of postsynaptic AMPA receptors. J Neurosci. 2008; 28:7820–7827. [PubMed: 18667614]

Zhao Y, Leal K, Abi-Farah C, Martin KC, Sossin WS, Klein M. Isoform specificity of PKC translocation in living Aplysia sensory neurons and a role for Ca2+-dependent PKC APL I in the induction of intermediate-term facilitation. J Neurosci. 2006; 26:8847–8856. [PubMed: 16928874]

Zhou G, Seibenhener ML, Wooten MW. Nucleolin is a protein kinase C-zeta substrate. Connection between cell surface signaling and nucleus in PC12 cells. J Biol Chem. 1997; 272:31130–31137. [PubMed: 9388266]

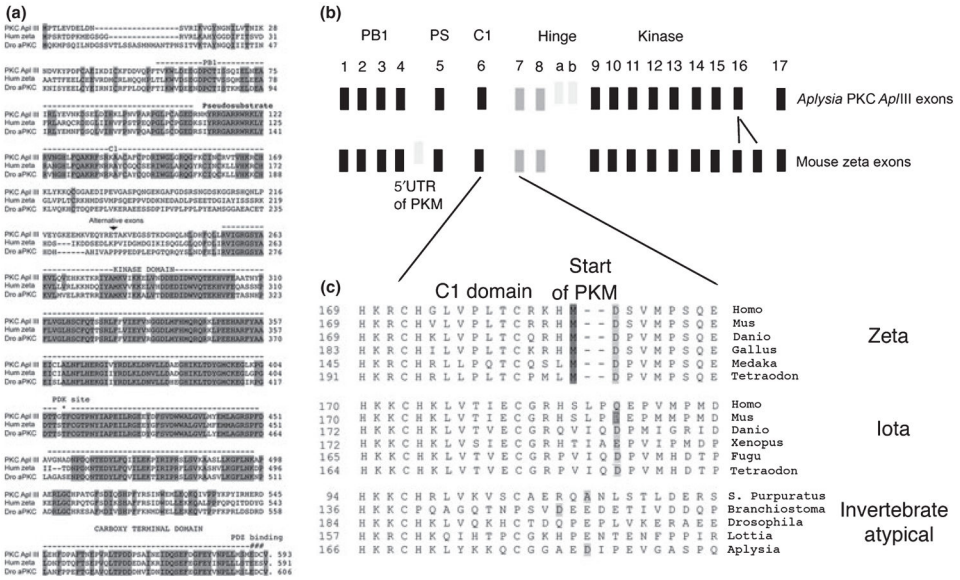

Fig. 1.

Cloning of PKC *Apl* III and evolution of the alternative transcript encoding PKMζ. (a) Sequence alignment of Human PKC zeta (Hum zeta), *Aplysia* PKC *Apl* III (PKC *Apl* III) and Drosophila atypical PKC (Dro aPKC). Amino acids conserved in all three are shaded. The domains are indicated by dotted lines over the regions. The phosphorylation sites are starred (*), as is a putative PDZ binding domain (###) at the C-terminal. The arrow indicates where alternative exons are inserted in *Aplysia* PKC *Apl* III. (b) Exon-intron structure of *Aplysia* PKC *Apl* III and Mouse zeta are shown. Black exons have conserved boundaries. The hinge exons 7 and 8 do not have conserved start and stop regions. In Mice, exon 16 is split into two exons. The positions of the alternative exons 8a and 8b in *Aplysia* and the position of the alternative transcriptional start site for PKMζ are indicated. (c) Alignment of the end of exon 6 and beginning of exon 7 in vertebrate and invertebrate sequences. All sequences from Genbank except for *Lottia* and *Brachiostoma* sequences that are from the Joint Genome Institute genome site (http://genome.jgi-psf.org). The methionine present in all vertebrate PKCζ is the last amino acid in exon 6 and occurs immediately following the end of the C1 domain. This methionine is not present in any PKCι or invertebrate PKCs including primitive deuterostomes such as *Branchiostoma* that have a single atypical form.

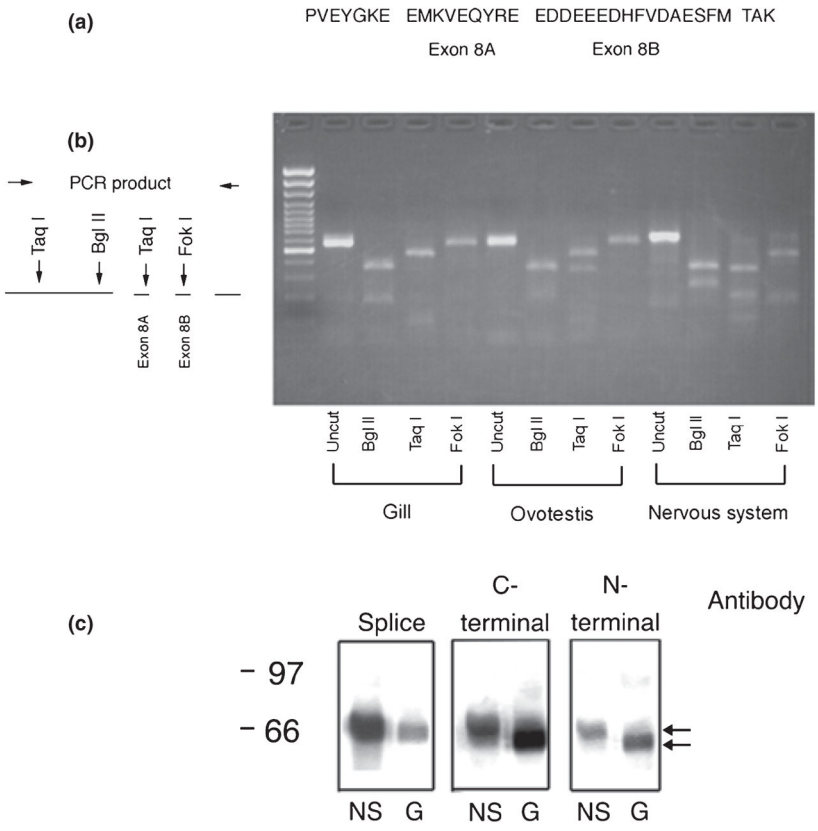

Fig. 2.

The splice inserts are enriched in nervous system PKC *Apl* III (a) Exon sequence of the alternative splice inserts (exon 8a and exon 8b) in the hinge domain of PKC *Apl* III. (b) Image of an agarose gel showing the results of digesting an amplified fragment of PKC *Apl* III cut with the restriction enzymes indicated. The product was amplified from cDNA isolated from Gill, Ovotestis or the Nervous System. A schematic of the placement of the restriction enzymes is shown on the left and the 100 bp marker is run in the left lane. (c) 20 μg of total protein extracted from either the Nervous System (NS) or Gill (G) were separated on SDS–PAGE gels, transferred to nitrocellulose and immunoblotted with the antibodies indicated.

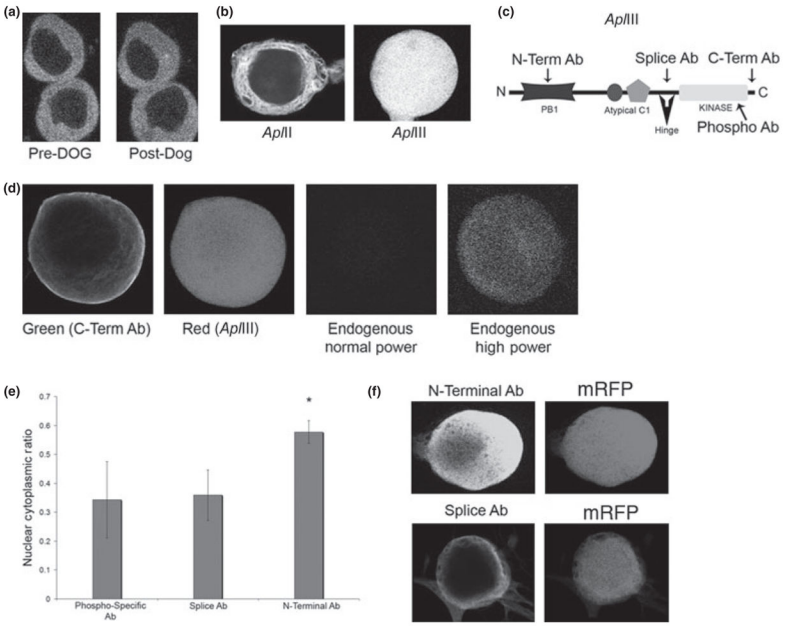

Fig. 3.

PKC *Apl* III is localized in nucleus and cleaved after expression in sensory neurons. (a) SF9 cells were transfected with mRFP-PKC *Apl* III and live images are shown of the red signal either before or after treatment with 50 μg/mL of dioctanoylglycerol. (b) Plasmids encoding either mRFP-PKC *Apl* II or mRFP-PKC *Apl* III were injected into sensory neurons, and the neurons were fixed 1 day later and imaged for mRFP. (c) Schematic of mRFP-*Apl* III with sites of the peptides used for antibody generation. (d) Plasmid encoding mRFP-PKC *Apl* III was injected into sensory neurons and neurons were fixed 1 day later and immunostained with the antibody to the C-terminal of PKC *Apl* III and simultaneously imaged for mRFP staining. The signal at the same laser power is shown for a non-injected neuron from the same preparation, as well as another image of the same neuron after increasing the laser power to image endogenous expression. (e) Quantification of sensory neurons expressing PKC *Apl* III immunostained with either the phospho-specific antibody ($n = 2$ experiments, 15 cells), the splice antibody ($n = 4$ experiments 17 cells), or the N-terminal antibody ($n = 3$ experiments, 24 cells). ANOVA revealed a significant difference between groups [$F(56,2) = 7.2$, $p < 0.01$] and Tukey's *post-hoc* test showed that the N-terminal antibody group was significantly different from both other groups (*, $p < 0.05$). (f) A representative example of neurons expressing mRFP-PKC *Apl* III immunostained with either the N-terminal antibody or the anti-splice antibody. mRFP fluorescence is shown on the right.

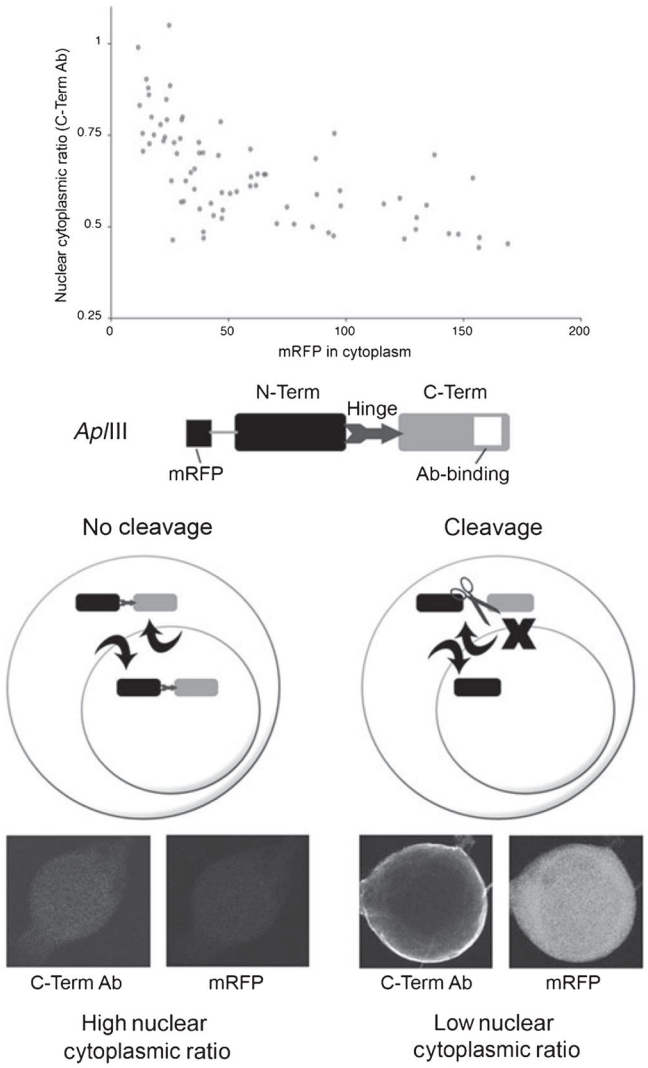

Fig. 4.

Model of the cleavage of PKC *Apl* III. Top: The correlation between the nuclear/cytoplasmc ratio (Y axis) and the level of expression (mRFP fluorescence in cytoplasm on X axis) is shown for a representative experiment. A similar pattern has been observed in over six experiments. *Apl* III construct with mRFP tag at the N-terminal and antibody site on C-Terminal, with hinge region linking the two. Bottom: At low expression levels, PKC *Apl* III is not cleaved and N-terminal (red) and C-terminal (green) remain linked shuttling together through the nucleus and cytoplasm. Sensory cells display a uniform pattern of red and green throughout the cell, resulting in a high nuclear/cytoplasmic ratio. At high expression levels, cleavage of PKC *Apl* III takes place in the hinge domain, dissociating the N-terminal (red) from the C-Terminal (green). The N-terminal continues to shuttle in and out of the nucleus, while the C-terminal remains restricted to the cytoplasm. Sensory cells display a red throughout the cell while the green is limited to the cytoplasm, resulting in a low nuclear/cytoplasmic ratio.

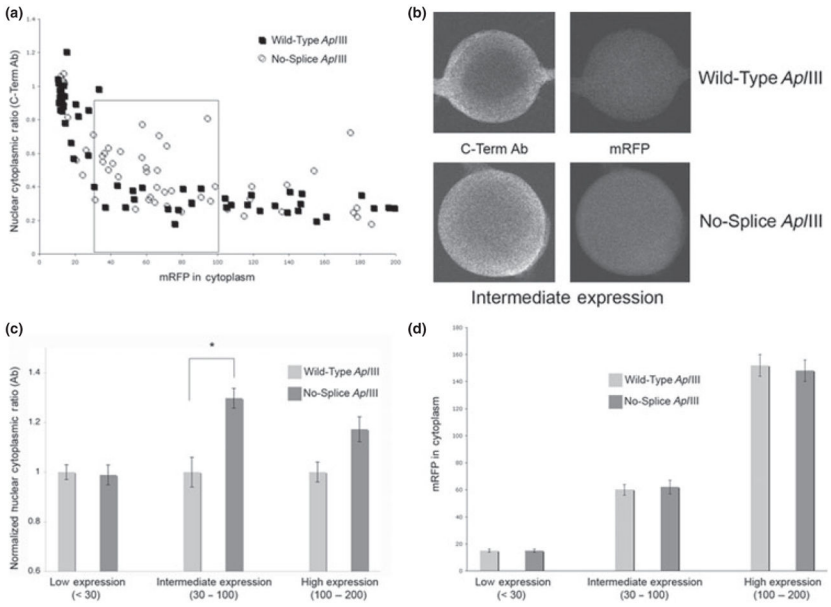

Fig. 5.

PKC *Apl* III cleavage is regulated by splicing. (a) The correlation between the nuclear/cytoplasmc ratio (Y axis) and the level of expression (mRFP fluorescence in cytoplasm on X axis) is shown for individual sensory neurons expressing mRFP-PKC *Apl* III Wild-Type (filled squares) or mRFP-PKC *Apl* III (No-Splice) (open circles). The region used to quantify differences in (c) is boxed. (b) A representative example of sensory neurons expressing Wild-Type mRFP-PKC *Apl* III (above) or No-Splice mRFP-PKC *Apl* III (below) immunostained with the antibody to the C-terminal (left) and imaged for mRFP fluorescence (right). (c) The average of the nuclear/cytoplasmic ratio stratified by the level of mRFP expression. Results are from three experiments: low expression, $n = 21$ (Wild-Type), 17 (No-Splice); intermediate expression, $n = 15$ (Wild-Type), 29 (No-Splice); and high expression, $n = 12$ (Wild-Type), 18 (No-Splice). $^{*}p < 0.03$ two-tailed Student's *t*-test. (d) Levels of mRFP expression in the three groups show no differences between mRFP-PKC *Apl* III Wild-Type and mRFP-PKC *Apl* III No-Splice that could explain the difference in the ratio.

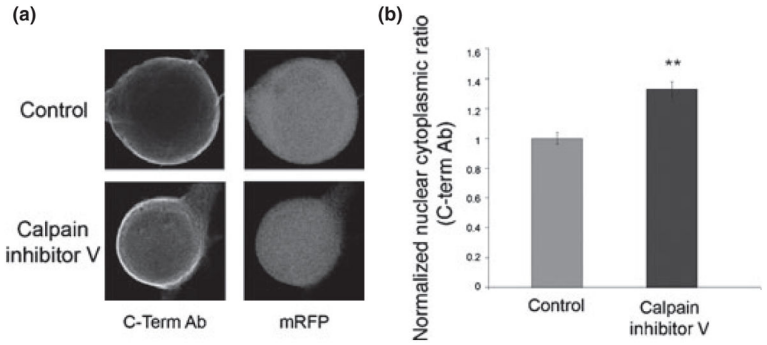

Fig. 6.

Cleavage is blocked by a calpain inhibitor. (a) Sensory neurons expressing mRFP-PKC *Apl* III were treated 1 h after plasmid injection with vehicle solution or Calpain Inhibitor V (100 μM), and then fixed 1 day later and immunostained with the carboxy-terminal antibody (left) or imaged for mRFP fluorescence (right). (b) Quantified results of the normalized nuclear/cytoplasmic ratio from three experiments (control, $n = 43$ cells, Calpain Inhibitor, $n = 74$ cells), $^{**}p < 0.001$ two tailed Student's *t*-test.

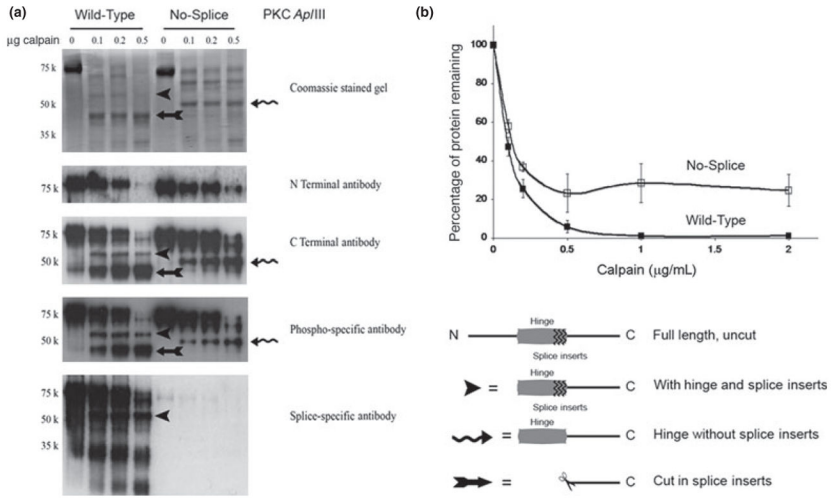

Fig. 7.

Calpain cleaves at the splice inserts *in vitro*. (a) PKC *Apl* III, with (Wild-Type) and without (No-Splice) the splice inserts, was purified from baculovirus and incubated with concentrations of purified calpain indicated. A representative experiment with 90% of the protein separated on one SDS–PAGE gel and stained with Coomassie, and 10% transferred to nitrocellulose and sequentially stained with the antibodies shown on the right, with stripping between each antibody incubation. Molecular weight markers are indicated on the left. Three bands are labeled with arrows (see schematic for description). Schematic of predicted bands based on molecular weight of PKC *Apl* III. (b) Quantification of cleavage for PKC *Apl* III Wild-Type or PKC *Apl* III No-Splice with each point from a total of 5–10 experiments.

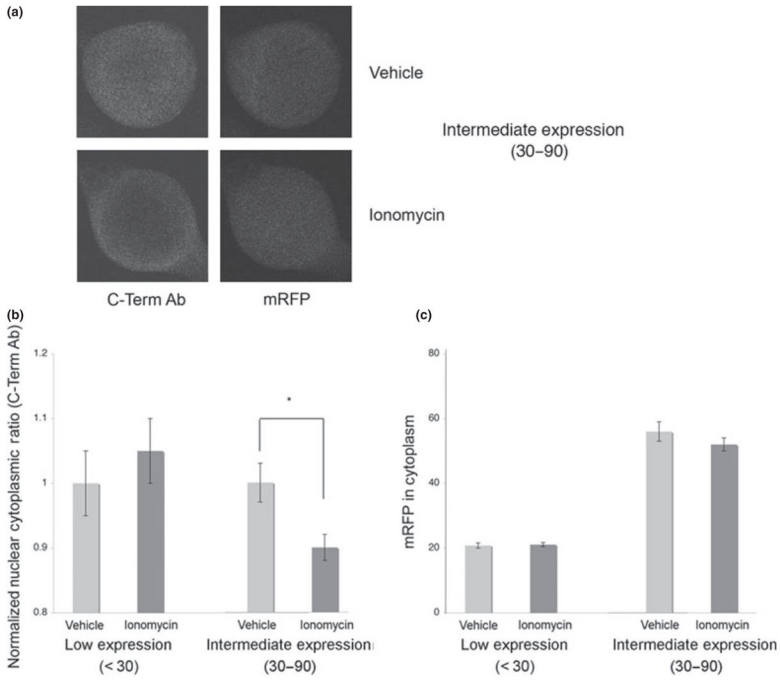

Fig. 8.

Ionomycin induced cleavage of PKC *Apl* III. (a) Sensory neurons over-expressing PKC *Apl* III were treated with a calcium ionophone, ionomycin (1 μM for 10 min), or a vehicle solution, fixed 2 h later and immunostained with the antibody to the carboxy-terminal (left) or imaged for mRFP (right). (b) Quantification of the nuclear/cytoplasmic ratio of control and ionomycin treated cells from three independent experiments (Cells > 30 and < 100 mRFP, Control, $n = 63$, ionomycin, $n = 71$; Cells < 30, Control, $n = 33$, ionomycin, $n = 54$) $^*p < 0.01$ Student's *t*-test between control and ionomycin.

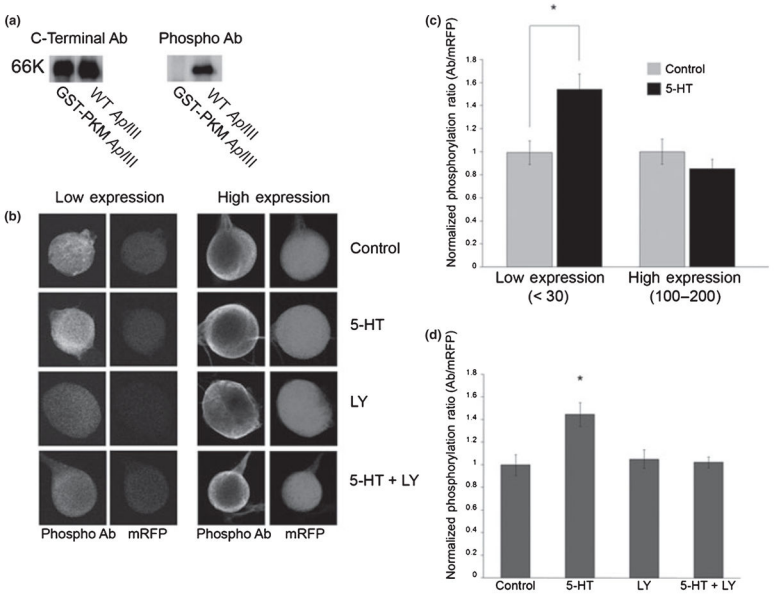

Fig. 9.

PKC *Apl* III phosphorylated at the PDK site is increased after 5HT treatment. (a) 10 ng of purified GST-catalytic domain and 50 ng of SF9 cell extract from cells infected with a baculovirus expressing PKM *Apl* III were separated on SDS–PAGE acrylamide gels, transferred to nitrocellulose, and immunostained with the antibody to the carboxyterminal (left) or the phospho-specific antibody to the PDK site (right). (b) Sensory cells over-expressing PKC *Apl* III were treated with either a control solution, 5HT (20 μM for 10 min), LY 294002 (10 μM for 10 min), or both LY and 5HT: LY (10 μM) was applied for 15 min prior to the 5HT (10 min) treatment. Cells were immediately fixed and immunostained with the phospho-specific antibody and imaged for mRFP. Examples are shown either at low levels of expression or high levels of expression. (c) Quantification of normalized phosphorylation ratio for low and high expressing neurons: low expression data from three experiments, C, $n = 14$, 5HT, $n = 22$, and high expression from two experiments, C, $n = 7$, 5HT, $n = 8$. *, $p < 0.05$ Students two-tailed paired *t*-test using non-normalized data. (d) Quantification of normalized phosphorylation after experimental treatments (C, five experiments, $n = 18$; 5HT, four experiments, $n = 44$; LY three experiments, $n = 12$; 5HT + LY three experiments, $n = 26$). ANOVA $F(96,3) = 8.9$, $p < 0.01$; Tukey's *post-hoc* test showed that 5HT was different from all other groups, *, $p < 0.05$ and no other differences were seen.